THE JOURNAL OF PHYSICAL CHEMISTRY B

Article

pubs.acs.org/JPCB

Assessment of the Use of NMR Chemical Shifts as Replica-Averaged Structural Restraints in Molecular Dynamics Simulations to Characterize the Dynamics of Proteins

Carlo Camilloni,[†] Andrea Cavalli,[†,‡] and Michele Vendruscolo[†]

[†]Department of Chemistry, University of Cambridge, Lensfield Road, Cambridge CB2 1EW, United Kingdom

[‡]Institute for Research in Biomedicine, Via Vincenzo Vela 6, 6500 Bellinzona, Switzerland

Supporting Information

ABSTRACT: It has been recently proposed that NMR chemical shifts can be used as replica-averaged structural restraints in molecular dynamics simulations to determine the conformational fluctuations of proteins. In this work, we assess the accuracy of this approach by considering its application to the case of ribonuclease A. We found that the agreement between experimental and calculated chemical shifts improves on average when the chemical shifts are used as replica-averaged restraints with respect to the cases in which X-ray structures or ensembles of structures obtained by standard molecular dynamics simulations are considered. These results indicate that the use of chemical shifts as structural restraints enables a bias of the conformational sampling to be introduced in a system-specific manner to reproduce accurately the conformational fluctuations of proteins.

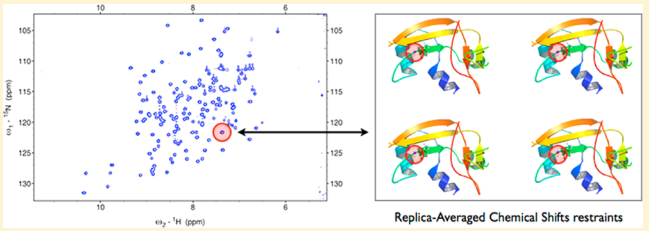

INTRODUCTION

As NMR chemical shifts are the results of time and ensemble averaged measurements, they contain, at least in principle, information about the structure and dynamics of the molecules under observation. Several methods have thus been proposed to use these parameters to characterize the conformational fluctuations of proteins.[1−14] In one of these approaches, molecular dynamics simulations are performed and the average chemical shifts are calculated from the resulting trajectories.[4,5,8−10] Detailed comparisons between experimental and calculated chemical shifts provide insights into the relationship between conformational fluctuations and chemical shifts.[4,5,8−10] In other approaches, the chemical shifts are incorporated as an additional term in the force field in the molecular dynamics simulations to enforce an agreement between experimental and calculated chemical shifts.[14,15] These methods exploit the power of molecular dynamics simulations to provide an accurate description of the thermodynamics and dynamics of proteins through the numerical integration of the equations of motion.[16−18] When the sampling of the conformational space is carried out to convergence, one obtains the Boltzmann weights corresponding to the force fields used, and hence a description of the associated free energy landscapes. If restrained molecular dynamics simulations are carried out, the experimental information provided by the chemical shifts is used to adapt the force field to reproduce the specific properties observed for the system under investigation.[14,15]

The question that we address here concerns the accuracy of these two approaches in describing the conformational fluctuations of proteins. If the force field used in the unrestrained molecular dynamics simulations is of high quality, the resulting description of the dynamics represents accurately the motions of proteins. However, even with state-of-the-art force fields differences between experimental and back-calculated chemical shifts are often observed.[4,5,8−10] These differences can be minimized by improving the force fields[8,19−21] or by directly incorporating the chemical shifts as structural restrains.[14,15] In the latter case, the equations of motion are integrated with an additional term in the force field that explicitly biases the trajectory toward conformations whose calculated chemical shifts match the experimental ones.[14,15] This approach, however, may suffer from a variety of potential problems. Despite recent advances,[10,22−27] current methods for calculating the chemical shifts corresponding to given structures are still of limited accuracy, thus providing an imperfect mapping between structures and chemical shifts. In addition, as the experimental chemical shifts are the results of a time and ensemble averaging procedure during the measurements, unless such averaging procedure is reproduced faithfully in the simulations, the resulting mapping between experimental and back-calculated chemical shifts would involve further inaccuracies.[5,8,10] The introduction of these types of systematic errors in the implementation of chemical shifts as structural restraints may effectively result in random forces in the sampling and in a description of structures and dynamics of comparable or even

Received: October 28, 2012
Revised: January 15, 2013
Published: January 16, 2013

lower accuracy than that of unrestrained molecular dynamics simulations.

To compare the accuracy of restrained and unrestrained molecular dynamics simulations in representing the information about conformational fluctuations provided by chemical shifts, we consider here the case of ribonuclease A (RNase A), a 124-residue protein whose structure and dynamics have been characterized in detail.[28−36] Our results indicate that the use of chemical shifts as replica-averaged structural restraints provides an effective method to characterize the dynamics of this protein.

METHODS

Structural Ensemble Extracted from the PDB (PDB Ensemble). We considered all the available X-ray structures for the free state of RNase A from the PDB, which were then protonated using the *Almost* molecular simulation package.[37,38]

Minimised PDB Ensemble (mPDB Ensemble). In this ensemble, the structures in the PDB ensemble described above were energy-minimized using *Almost*[37,38] to optimise the local geometry and remove structural clashes.

Molecular Dynamics Simulations. All of the molecular dynamics simulations in the present work were performed using *Gromacs*.[39] Unless stated otherwise, all of the simulations were carried out using the Amber99SB*-ILDN force field[40] and the TIP3P water model.[41] A time step of 2 fs was used together with LINCS constraints.[39] The van der Waals interactions were cutoff at 1.2 nm, and long-range electrostatic effects were treated with the particle mesh Ewald method.[42] All of the simulations were done in the canonical ensemble by keeping the volume fixed and by thermosetting the system with the Bussi thermostat.[43] The starting conformation was taken from an X-ray structure[28] (PDB code 1JVT). This structure was protonated and solvated with 6302 water molecules in a dodecahedron box of 208.6 nm^3 of volume. The energy of the system was first minimized and then the temperature was increased to 300 K in two separate steps, in the first one a 50 ps long simulation was performed by keeping fixed the heavy atoms of the protein, and successively a second 200 ps long simulation was performed without restraints. The density of the system has been relaxed by a 200 ps long run using the Berendsen barostat.[44]

Structural Ensemble Obtained Using Unrestrained Molecular Dynamics Simulations (MD Ensemble). A 250 ns simulation was performed at 300 K to sample the native state dynamics of RNase A. The structures sampled in the last 240 ns were used for the analysis of the dynamics.

Structural Ensemble Obtained Using Molecular Dynamics Simulations with Replica-Averaged Chemical Shift Restraints (CS-MD Ensemble). We optimized the number of replicas after changing the form of the scoring function with respect to previous studies[14,15] by removing the flat bottom potential. The new scoring function is a sum of parabolic functions

$$E_{CS} = \sum_{N}^{i=1} \sum_{6}^{j=1} (\delta_{ij}^{calcd} - \delta_{ij}^{exp\,t})^2$$

where j is the atom type (i.e., Hα, HN, N, Cα, Cβ, and C′) in the ith residue of a protein of length N. The rationale of using this simplified functional form instead of the flat bottom potential used in previous studies is 2-fold. On the one hand, the calculated chemical shifts should always correspond to the most probable values, and a flat bottom potential does not represent correctly this probability. On the other hand, the flat bottom potential prevents over-restraining in the case of simulations in which all of the restraints are applied on a single replica.[14,15] Because, however, here the over-restraining is avoided by using multiple replicas,[14,45,46] it is not necessary to use the flat bottom potential.

We carried out molecular dynamics simulations with replica-averaged chemical shift restraints, using four replicas. The starting structures for the four replicas were selected as the final structure from four 1 ns simulations. Experimental chemical shifts were taken from the BMRB 4031 entry[47] and applied as restraints over the four replicas of the system. *CamShift*[23] was used to calculate the chemical shifts from all of the replicas at each time step. Each replica was evolved through a series of annealing cycles between 300 K and 400 K, each cycle being composed of 100 ps at 300 K, 100 ps of linear increase in the temperature up to 400 K, 100 ps of constant temperature molecular dynamics simulations at 400K and 300 ps of linear decrease in the temperature to 300 K. Only structures from the 300 K portions of the simulations were taken into account for analysis. Each replica was evolved for 50 ns. The resulting ensemble is composed by all of the structures sampled at 300 K by all of the replicas. The structural restraints were added to *Gromacs* by using *PLUMED*[48] and *Almost*.[37,38]

Test of the Reference Ensemble. The test of the reference ensemble was performed following a previously described procedure[14] and the results are presented in detail in the Supporting Information. The conclusion of this test is that by removing the flat bottom potential the optimal number of replicas increases to 4, with results that are better in reproducing the reference ensemble of those obtained in previous publications by using 2 replicas and the flat bottom potential.

Structure-Based Calculation of the Chemical Shifts. In all cases (MD ensemble, CS-MD ensemble, PDB ensemble, and mPDB ensemble), we used *Sparta+*[24] to calculate the chemical shifts from the structures. For the generation of the CS-MD ensemble, we used *CamShift*[23] within the molecular dynamics simulations with replica-averaged chemical shift restraints to calculate the chemical shifts and their derivatives. *Sparta+*[24] and *CamShift*[23] perform structure-based prediction of chemical shifts of proteins using phenomenological approaches that capture in an approximate manner the conformational dependence of the chemical shifts themselves. The accuracy of the methods is of the order of 1 ppm for carbon atoms, 2.5 ppm for nitrogen atoms, and 0.3 for hydrogen atoms.

RESULTS AND DISCUSSION

Molecular Dynamics Simulations. We generated two ensembles of structures representing the conformational dynamics in the native state of RNase A. The first ensemble (MD ensemble) was determined by unrestrained molecular dynamics simulations (Methods), while the second ensemble (CS-MD ensemble) was determined using molecular dynamics simulations with replica-averaged chemical shift restraints (Methods).

Comparison between Experimental and Calculated Chemical Shifts. To quantify the agreement between experimental and calculated chemical shifts, we considered the average error for each atom type (Figure 1). In the case of the PDB and mPDB ensembles, we report the average error of

dx.doi.org/10.1021/jp3106666 | J. Phys. Chem. B 2013, 117, 1838−1843

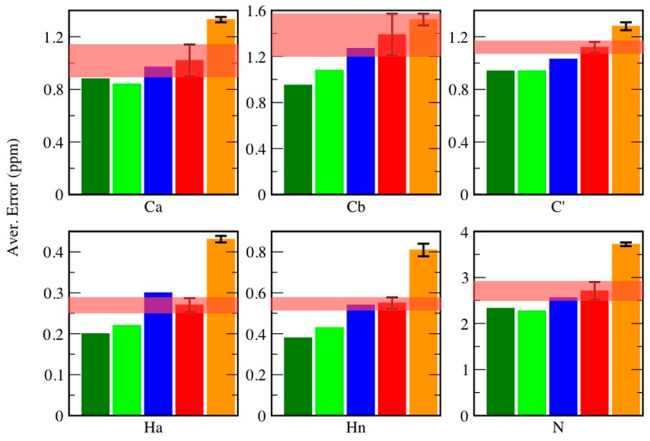

Figure 1. Comparison of the differences between experimental and calculated chemical shifts for the ensembles considered in this study. Green bars represent the CS-MD ensemble, blue bars the MD ensemble, red and orange bars the PDB ensemble after (mPDB ensemble) and before (PBD ensemble) energy minimization, respectively; the orange-shaded band represents the standard error in the chemical shifts of the mPDB ensemble. The differences are given in ppm and represent the root-mean-square distance between the experimental and the calculated chemical shifts.

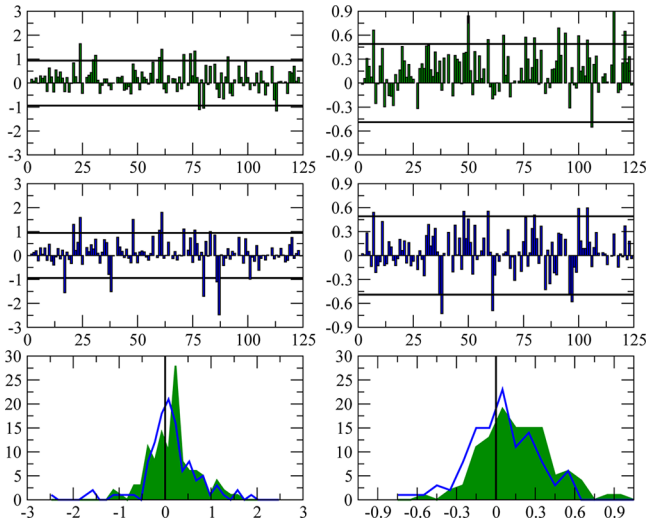

Figure 2. Residue-by-residue analysis of the $|\delta$X-ray $- \delta$Exp$| - |\delta$Ens $- \delta$Exp$|$ values[9] for Cα carbon (left column) and HN hydrogen (right column) atoms (values are given in ppm). The results for the CS-MD ensemble are shown in the top panels, and the results for the MD ensemble in the central panels. In the bottom panels we compare the distributions of the above panels.

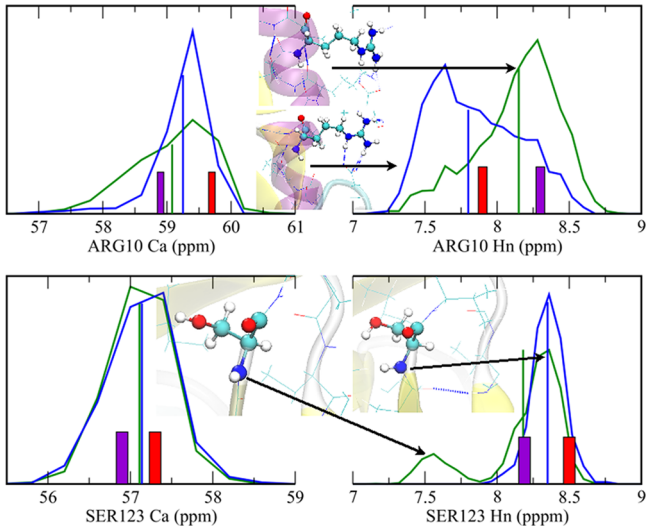

Figure 3. Analysis of the distributions of the Cα and H chemical shifts for Arg10 (top panel) and Ser123 (bottom panel). Green lines refer to the CS-MD ensemble, blue lines to the MD ensemble, red bars represent the 1JVT crystal structure, and violet bars the measured experimental chemical shifts. Representative corresponding structures are also shown.

the calculated chemical shifts, while in the cases of the MD and CS-MD ensembles the error of the average chemical shifts. Chemical shifts were calculated from the structures in all cases using *Sparta+*.[24] In the case of RNase A, we found that, on average, the MD ensemble (blue bars in Figure 1) exhibits a comparable agreement with the experimental chemical shifts with respect to the set of minimized crystal structures (the mPDB ensemble, red bars). By contrast, we found that on average the agreement between experimental and calculated chemical shifts for the CS-MD ensemble (green bars represent an ensemble previously published[14] and dark green bars the present ensemble) is about one standard deviation better than for the mPDB ensemble. These results indicate that the use of chemical shifts as replica-averaged structural restraints enables one to capture the dynamic information provided by the chemical shifts.

A more detailed analysis at the individual residue level is useful to evaluate the degree to which an ensemble of conformations captures the information about the dynamics present in the chemical shifts.[9] We performed a residue-by-residue analysis of the $|\delta$X-ray $- \delta$Exp$| - |\delta$Ens $- \delta$Exp$|$ values for Cα carbon and HN hydrogen atoms (Figure 2). Positive values indicate residues for which the CS-MD ensemble is in better agreement with the experimental chemical shifts than the energy-minimized crystal structure (in this case 1JVT), whereas negative values are for those residues for which the CS-MD ensemble is in poorer agreement. The black horizontal line represents the average error of *Sparta+* and indicates the level of significance. The distributions are on average better for the CS-MD ensemble than for the MD ensemble, and in particular the addition of the replica-averaged chemical shifts restraints appears to be able to correct the dynamics of those residues whose conformational fluctuations are not described well by the force-field that we used in this work (Figure 2).

Analysis of Individual Residues. Further insights can be obtained by looking at the behavior of specific residues. We first considered the cases of Arg10 and Ser123 (Figure 3). In both of these cases, an averaging between different conformations is needed to reproduce the experimental chemical shifts. Such an averaging, however, is not captured by the MD ensemble. In particular in the case of Arg10, the experimental chemical shifts (58.9 and 8.3 ppm Cα carbon and HN chemical shifts, respectively) are far from the one of the X-ray structure (59.7 and 7.9 ppm). The CS-MD ensemble is in better agreement with the experimental values (59.1 and 8.1 ppm) and results in a distribution of structures in which Arg10 is in equilibrium between two different conformations of the α-helix characterized by a hydrogen bond between residues 6 and 10 that can be stronger or weaker (Figure 3). This feature results in a bimodal distribution of the HN chemical shifts, which are directly involved in the hydrogen bond, and a single peak

dx.doi.org/10.1021/jp3106666 | J. Phys. Chem. B 2013, 117, 1838−1843

distribution of the Cα carbon, which is more sensitive to the local backbone. The MD ensemble explores almost the same range of conformations but with different statistical weights, resulting in chemical shifts that are more similar to the X-ray ones (59.3 and 7.8 ppm). For Ser123 the behavior is similar, in that the experimental chemical shifts (56.9 and 8.2 ppm Cα carbon and HN chemical shifts, respectively) are far from that of the X-ray structure (57.3 and 8.5 ppm). The CS-MD ensemble is in better agreement with the experimental values (57.1 and 8.2 ppm) and results in a distributions of structures in which Ser123 is in equilibrium between a major and a minor conformation of the backbone. In the most populated one, the backbone of Ser123 adopts a planar conformation that helps the stabilization of the final tail of the last β-strand, with the preceding residue 122 that can form a hydrogen bond. In the minor conformation, the planar organization of the backbone is lost and also the preceding hydrogen bond is broken (Figure 3). This fact results in a bimodal distribution of the HN chemical shifts, while the Cα chemical shifts are normally distributed. In this case the MD ensemble explores only the most populated conformer, the one more similar to the X-ray structure, without capturing the equilibrium with the minor conformation, with chemical shifts in worst agreement with the experimental ones (57.1 and 8.4 ppm). These two cases illustrate how the use of the chemical shift averaging, by improving the agreement with the experimental data, could provide insights into the underlying conformational fluctuations.

We also considered cases in which the improvement with respect to the MD ensemble is not significant (Figure 2). In particular, in the case of Ser80, the Cα chemical shifts measured experimentally and those calculated from the minimized X-ray structure are in essentially perfect agreement (56.9 ppm in both cases), while the average value of both the CS-MD and the MD ensembles are quite different (58.0 ppm and 58.6 ppm respectively). In order to understand the structural features associated with these results we considered the distributions of the chemical shifts in the two ensembles and the distribution of the φ dihedral angle of Ser80 (Figure 4). This example illustrates how a specific residue can be directed by the force field toward an incorrect region of the Ramachandran space,

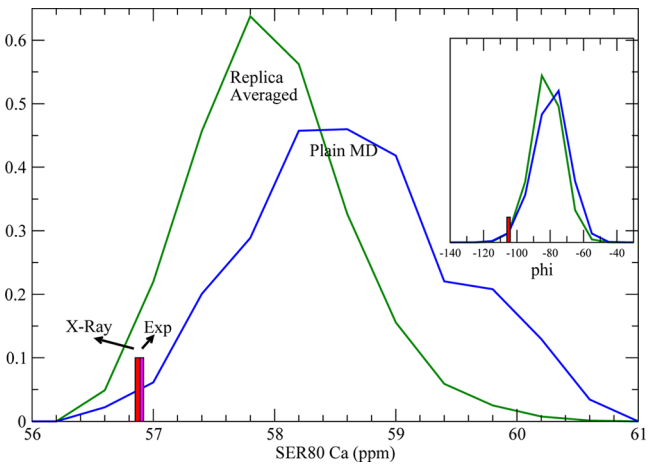

Figure 4. Analysis of the distribution of chemical shift values for the Ser80 Cα atom in the MD ensemble (Plain MD) and in the CS-MD ensemble (Replica Averaged). The inset shows the distributions of the phi dihedral angle of Ser80 in the two ensembles.

and also how the chemical shift restraints are partially successful in correcting this effect. Next, we consider a situation in which the experimental chemical shifts are not in agreement with the minimized X-ray structure (Asn113, Figure 5). In this case, also

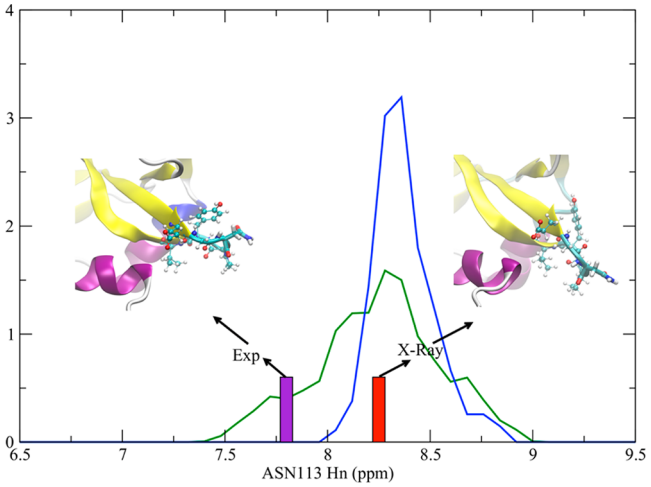

Figure 5. Analysis of the distribution of chemical shift values for the Asn113 HN atom in the different ensembles considered in this work.

the MD ensemble does not capture the dynamics of the residue and of its surrounding region, either for lack of sampling or for the quality of the force field (Figure 5); the average value of the HN chemical shift of Asn113 is 8.4 ppm in the MD ensemble, which is very similar to that of the X-ray structure (8.3 ppm), with a single-peaked distribution. The CS-MD ensemble shows instead a double-peaked distribution, with an average value of 8.2 ppm, which is in better agreement with the experimental value of 7.8 ppm. In particular, both the MD and CS-MD ensembles have a peak that is structurally similar to the X-ray structure but, in the case of the CS-MD ensemble, the distribution of structures is broader with structures in which the Asn113 and the whole loop to which it belongs is farther from the first α-helix and with a different orientation of Tyr115. Thus, the addition of the chemical shifts as replica-averaged structural restraints, by increasing the agreement between experimental and back-calculated chemical shifts, can correct both the structural and the dynamical features of the underlying force field.

Analysis of Global Properties. In addition to the conformational properties of individual residues, it is of interest to look at the overall dynamical behavior of RNase A in its native state. The dynamics of RNase A in the free state is characterized by an equilibrium between a minor and a major conformers of the active site.[28−36] Both the conformers are present among the X-ray structures (PDB ensemble) and these where used to plot a free energy surface that represents this equilibrium in the case of the CS-MD ensemble. In particular, the conformers of both the major and the minor state had a root-mean-square distance (rmsd) of less than 1.5 Å from their relative X-ray structure. In the case of the MD ensemble, a similar equilibrium can be found and represented in term of free energy surfaces (Figure 6) but the ensemble covers a smaller conformational space and the relative statistical weights of the minima are different. From the experimental work of Loria and co-workers it is known that the minor conformer should account for around the 5% of the total population.[34] In the MD ensemble the minor conformer (Figure 6) accounts for

dx.doi.org/10.1021/jp3106666 | J. Phys. Chem. B 2013, 117, 1838−1843

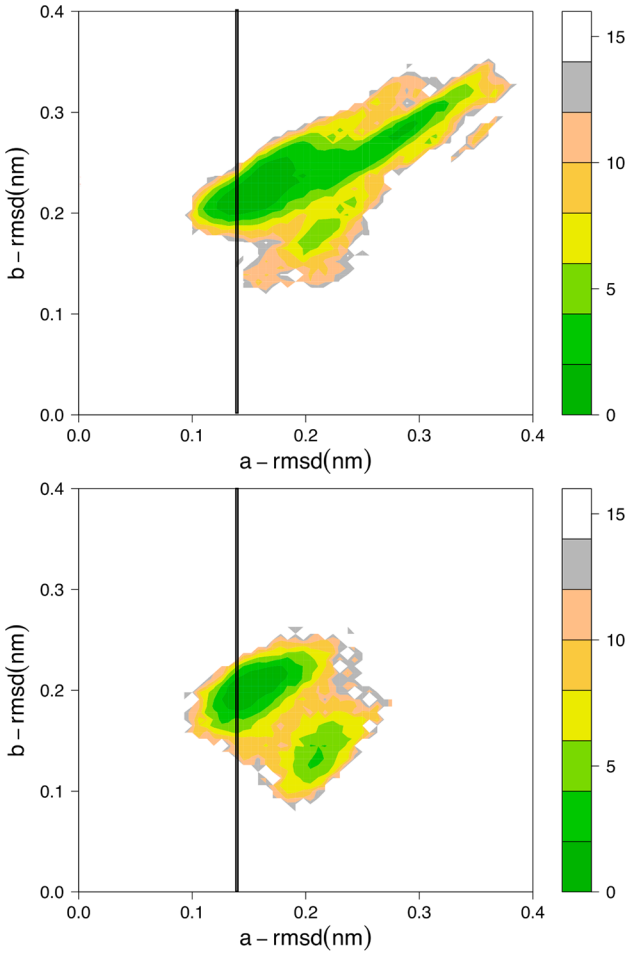

Figure 6. Free energy landscape of RNase A. By using chemical shift restraints (upper panel, CS-MD ensemble) we found two most populated clusters of structures, corresponding to the A state and the B state.[14] A different conformational equilibrium was found from the MD ensemble, where the two states exhibit a larger rmsd from the corresponding PDB structures. The two order parameters used to represent the free energy landscape correspond to the rmsd between the conformations in the ensemble that we generated and those available in the PDB (PDB ensemble) in the A (a-rmsd) and B (b-rmsd) states, respectively. The energy is in kJ/mol, with isolines every 2 kJ/mol.

the 22% of the total, whereas in the CS-MD ensemble the minor conformer accounts for only the 6% of the total.

CONCLUSIONS

We have shown that the use of NMR chemical shifts as replica-averaged structural restraints in molecular dynamics simulations of RNase A results in an ensemble of conformations that describe accurately the dynamics of this protein. This result is achieved by enforcing a better agreement between experimental and calculated chemical shifts with respect to that provided by the force field alone. Thus, the incorporation of chemical shifts as structural restraints within the molecular dynamics approach described here captures better than standard molecular dynamics simulations the structural and the dynamical information provided by the chemical shifts and improves the description of the conformational fluctuations of proteins. These results also indicate that the experimental NMR fingerprints of a protein are better reproduced by an average over an ensemble of structures covering a relatively large part of the conformational space, rather than by a given single conformation, as for example an optimized structure.

ASSOCIATED CONTENT

Supporting Information

Description of the reference ensemble test, and comparisons of the distributions of the interatomic distances (S matrix) in the restrained and unrestrained ensembles. This material is available free of charge via the Internet at http://pubs.acs.org.

AUTHOR INFORMATION

Notes

The authors declare no competing financial interest.

ACKNOWLEDGMENTS

C.C. was supported by a Marie Curie Intra European Fellowship, A.C. and M.V. by the BBSRC and the Wellcome Trust.

REFERENCES

(1) Hoch, J. C.; Dobson, C. M.; Karplus, M. *Biochemistry* **1982**, *21*, 1118−1125.
(2) Evans, P. A.; Topping, K. D.; Woolfson, D. N.; Dobson, C. M. *Proteins* **1991**, *9*, 248−266.
(3) Berjanskii, M. V.; Wishart, D. S. *J. Am. Chem. Soc.* **2005**, *127*, 14970−14971.
(4) Markwick, P. R. L.; Cervantes, C. F.; Abel, B. L.; Komives, E. A.; Blackledge, M.; McCammon, J. A. *J. Am. Chem. Soc.* **2010**, *132*, 1220−1221.
(5) De Gortari, I.; Portella, G.; Salvatella, X.; Bajaj, V. S.; van der Wel, P. C. A.; Yates, J. R.; Segall, M. D.; Pickard, C. J.; Payne, M. C.; Vendruscolo, M. *J. Am. Chem. Soc.* **2010**, *132*, 5993−6000.
(6) Hansen, D. F.; Kay, L. E. *J. Am. Chem. Soc.* **2011**, *133*, 8272−8281.
(7) Wishart, D. S. *Prog. Nucl. Mag. Res. Spec.* **2011**, *58*, 62−87.
(8) Li, D. W.; Bruschweiler, R. *J. Chem. Theor. Comp.* **2011**, *7*, 1773−1782.
(9) Robustelli, P.; Stafford, K. A.; Palmer, A. G. *J. Am. Chem. Soc.* **2012**, *134*, 6365−6374.
(10) Lehtivarjo, J.; Tuppurainen, K.; Hassinen, T.; Laatikainen, R.; Perakyla, M. *J. Biomol. NMR* **2012**, *52*, 257−267.
(11) Kjaergaard, M.; Poulsen, F. M. *Prog. Nucl. Mag. Res. Spec.* **2012**, *60*, 42−51.
(12) Markwick, P. R. L.; Nilges, M. *Chem. Phys.* **2012**, *396*, 124−134.
(13) Camilloni, C.; De Simone, A.; Vranken, W. F.; Vendruscolo, M. *Biochemistry* **2012**, *51*, 2224−2231.
(14) Camilloni, C.; Robustelli, P.; De Simone, A.; Cavalli, A.; Vendruscolo, M. *J. Am. Chem. Soc.* **2012**, *134*, 3968−3971.
(15) Robustelli, P.; Kohlhoff, K.; Cavalli, A.; Vendruscolo, M. *Structure* **2010**, *18*, 923−933.
(16) Karplus, M.; McCammon, J. A. *Nat. Struct. Biol.* **2002**, *9*, 646−652.
(17) Shaw, D. E.; Maragakis, P.; Lindorff-Larsen, K.; Piana, S.; Dror, R. O.; Eastwood, M. P.; Bank, J. A.; Jumper, J. M.; Salmon, J. K.; Shan, Y. B.; et al. *Science* **2010**, *330*, 341−346.
(18) Vendruscolo, M.; Dobson, C. M. *Curr. Biol.* **2011**, *21*, R68−R70.
(19) Lindorff-Larsen, K.; Maragakis, P.; Piana, S.; Eastwood, M. P.; Dror, R. O.; Shaw, D. E. *PLoS One* **2012**, *7*.
(20) Best, R. B. *Curr. Op. Struct. Biol.* **2012**, *22*, 52−61.
(21) Nielsen, J. T.; Eghbalnia, H. R.; Nielsen, N. C. *Prog. Nucl. Mag. Res. Spec.* **2012**, *60*, 1−28.
(22) Xu, X. P.; Case, D. A. *J. Biomol. NMR* **2001**, *21*, 321−333.
(23) Kohlhoff, K. J.; Robustelli, P.; Cavalli, A.; Salvatella, X.; Vendruscolo, M. *J. Am. Chem. Soc.* **2009**, *131*, 13894−13895.
(24) Shen, Y.; Bax, A. *J. Biomol. NMR* **2010**, *48*, 13−22.
(25) Han, B.; Liu, Y. F.; Ginzinger, S. W.; Wishart, D. S. *J. Biomol. NMR* **2011**, *50*, 43−57.

(26) Sahakyan, A. B.; Vranken, W. F.; Cavalli, A.; Vendruscolo, M. *J. Biomol. NMR* **2011**, *50*, 331−346.
(27) Sahakyan, A. B.; Vranken, W. F.; Cavalli, A.; Vendruscolo, M. *Angew. Ch. Int. Ed.* **2011**, *50*, 9620−9623.
(28) Vitagliano, L.; Merlino, A.; Zagari, A.; Mazzarella, L. *Proteins* **2002**, *46*, 97−104.
(29) Beach, H.; Cole, R.; Gill, M. L.; Loria, J. P. *J. Am. Chem. Soc.* **2005**, *127*, 9167−9176.
(30) Cole, R.; Loria, J. P. *Biochemistry* **2002**, *41*, 6072−6081.
(31) Doucet, N.; Khirich, G.; Kovrigin, E. L.; Loria, J. P. *Biochemistry* **2011**, *50*, 1723−1730.
(32) Doucet, N.; Watt, E. D.; Loria, J. P. *Biochemistry* **2009**, *48*, 7160−7168.
(33) Kovrigin, E. L.; Cole, R.; Loria, J. P. *Biochemistry* **2003**, *42*, 5279−5291.
(34) Kovrigin, E. L.; Loria, J. P. *J. Am. Chem. Soc.* **2006**, *128*, 7724−7725.
(35) Kovrigin, E. L.; Loria, J. P. *Biochemistry* **2006**, *45*, 2636−2647.
(36) Watt, E. D.; Shimada, H.; Kovrigin, E. L.; Loria, J. P. *Proc. Natl. Acad. Sci. U.S.A.* **2007**, *104*, 11981−11986.
(37) Cavalli, A.; Vendruscolo, M.; Paci, E. *Bioph. J.* **2005**, *88*, 3158−3166.
(38) Paci, E.; Cavalli, A.; Vendruscolo, M.; Caflisch, A. *Proc. Natl. Acad. Sci. U.S.A.* **2003**, *100*, 8217−8222.
(39) Hess, B.; Kutzner, C.; van der Spoel, D.; Lindahl, E. *J. Chem. Theor. Comp.* **2008**, *4*, 435−447.
(40) Lindorff-Larsen, K.; Piana, S.; Palmo, K.; Maragakis, P.; Klepeis, J. L.; Dror, R. O.; Shaw, D. E. *Proteins* **2010**, *78*, 1950−1958.
(41) Jorgensen, W. L.; Chandrasekhar, J.; Madura, J. D.; Impey, R. W.; Klein, M. L. *J. Chem. Phys.* **1983**, *79*, 926−935.
(42) Essmann, U.; Perera, L.; Berkowitz, M. L.; Darden, T.; Lee, H.; Pedersen, L. G. *J. Chem. Phys.* **1995**, *103*, 8577−8593.
(43) Bussi, G.; Donadio, D.; Parrinello, M. *J. Chem. Phys.* **2007**, *126*, 014101.
(44) Berendsen, H. J. C.; Postma, J. P. M.; Vangunsteren, W. F.; Dinola, A.; Haak, J. R. *J. Chem. Phys.* **1984**, *81*, 3684−3690.
(45) Lindorff-Larsen, K.; Best, R. B.; DePristo, M. A.; Dobson, C. M.; Vendruscolo, M. *Nature* **2005**, *433*, 128−132.
(46) Richter, B.; Gsponer, J.; Varnai, P.; Salvatella, X.; Vendruscolo, M. *J. Biomol. NMR* **2007**, *37*, 117−135.
(47) Shimotakahara, S.; Rios, C. B.; Laity, J. H.; Zimmerman, D. E.; Scheraga, H. A.; Montelione, G. T. *Biochemistry* **1997**, *36*, 6915−6929.
(48) Bonomi, M.; Branduardi, D.; Bussi, G.; Camilloni, C.; Provasi, D.; Raiteri, P.; Donadio, D.; Marinelli, F.; Pietrucci, F.; Broglia, R. A.; et al. *Comput. Phys. Commun.* **2009**, *180*, 1961−1972.